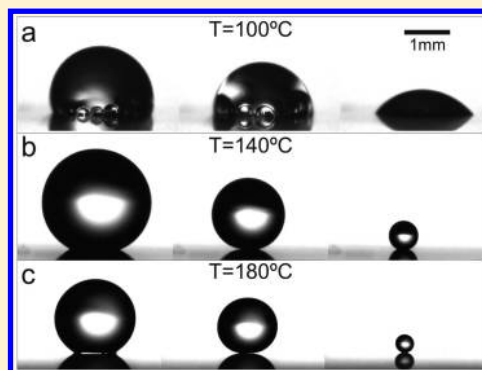


## Leidenfrost Point Reduction on Micropatterned Metallic Surfaces

Daniel Arnaldo del Cerro,<sup>\*,†</sup> Álvaro G. Marín,<sup>‡</sup> Gertwillem R. B. E. Römer,<sup>†</sup> B. Pathiraj,<sup>†</sup> Detlef Lohse,<sup>‡</sup> and Albertus J. Huis in 't Veld<sup>†</sup><sup>†</sup>Applied Laser Technology, Faculty of Engineering Technology and <sup>‡</sup>Physics of Fluids, MESA+ Institute for Nanotechnology, University of Twente, Enschede, The Netherlands

**ABSTRACT:** Droplets are able to levitate when deposited over a hot surface exceeding a critical temperature. This is known as the Leidenfrost effect. This phenomenon occurs when the surface is heated above the so-called Leidenfrost point (LFP), above which the vapor film between the droplet and hot surface is able to levitate the droplet. Such a critical temperature depends on several factors. One of the most studied parameters has been the surface roughness. Almost all of the experimental studies in the literature have concluded that the LFP increases with the roughness. According to these results, it seems that the roughness is detrimental for the stability of the vapor film. In contrast with these results, we present here a micropatterned surface that significantly reduces the LFP. The temperature increase, relative to the boiling point, required to reach the LFP is 70% lower than that on the flat surface. The reasons for such an effect are qualitatively and quantitatively discussed with a simple semiempirical model. This result can be relevant to save energy in applications that take advantage of the Leidenfrost effect for drop control or drag reduction.



## ■ INTRODUCTION

A liquid drop deposited over a surface at a temperature sufficiently above the liquid saturation point does not experience a sudden boiling. Instead, the droplet floats over a vapor layer that prevents the liquid from boiling. The vapor layer completely prevents contact between the liquid and the heated surface and therefore provides thermal isolation. In this situation, the droplet lacks any contact and friction with the solid, and thus, the so-called “Leidenfrost state” is often considered as a perfect superhydrophobic state. To reach such a state, the surface temperature has to reach a critical value known as the Leidenfrost point (LFP),<sup>1</sup> which has often been related and identified to the onset temperature for film boiling.<sup>2,3</sup>

The heat flux that is transferred from a heated surface in contact with a liquid keeps increasing with the wall temperature. At a given point above the liquid saturation point, the heat flux reaches a maximum, known as the critical heat flux (CHF). From this point, and due to the formation of an isolating vapor film, the heat flux starts to decrease. When the film is fully developed, the liquid is not in contact with the heated surface, and therefore, the heat flux reaches a minimum. The temperature at the minimum heat flux has been traditionally employed to determine the LFP.<sup>3,4</sup> This critical point has been shown to be highly dependent on several factors, such as the surface thermal properties, its roughness,<sup>5</sup> the drop size,<sup>6</sup> the method of drop deposition,<sup>7</sup> and so forth.

The Leidenfrost effect is of relevance for practical applications. On one hand, the effect has a clear detrimental influence on heat transfer, and therefore has to be taken into account when using liquids to cool down heated surfaces. In

this context, extensive research has been performed on both the theoretical and practical sides to make predictions on the LFP, with the attendant difficulties due to the number of parameters involved. Experimental studies were mainly focused on methods to increase the LFP of a system, which would give a wider dynamic range for cooling applications. Several authors have reported that the roughness of the surface substantially increases the LFP.<sup>3,8,9</sup> Classically, this has been done by etching or sandblasting the surface, giving it a random micro- or nanoroughness. More recently, Kim et al. have studied the effect of sparse surface microdefects on the LFP and the stability of the Leidenfrost state.<sup>10</sup>

On the other hand, the effect can be interesting to study, as it provides a perfect hydrophobic state lacking any contact with the surface. For this reason, the droplet moves freely following the slope of the surface until an obstacle is found. Recent studies with designed micropatterned surfaces were able to control the movement of the Leidenfrost drop.<sup>11–14</sup> Other studies have used the effect to reduce the drag of a heated metallic object immersed in a liquid, achieving reduction of drag coefficients up to 40%.<sup>15</sup> Another potential application would be to use the effect as a controlled droplet evaporation technique for evaporating complex droplets: to produce capsules on demand.<sup>16</sup> For such applications, it is therefore interesting to find ways to reduce the LFP and be able to reach such a state by using the least energy possible.

Received: May 29, 2012

Revised: September 24, 2012

Published: September 29, 2012

In this paper, we report a transition into a hydrophobic state with similar characteristics as the Leidenfrost state on a regular micropatterned surface, which occurs at temperatures significantly lower than the LFP on the flat surface. The temperature increase, relative to the boiling point, required to reach the LFP is 70% lower than that on the flat surface. This has been performed by using micropatterned metallic substrates with different surface structure morphologies. The liquid employed in the study is deionized water and the material is stainless steel (AISI 304 L).

## EXPERIMENTAL SECTION

A picosecond pulsed laser source was employed for the generation of the microstructures by direct material removal. By surface micropatterning with short laser pulses in the picosecond regime, a well-controlled surface topography can be created on a variety of substrates, with resolution typically in the micrometer range.<sup>17,18</sup>

The laser source operates at a central wavelength of 1030 nm and delivers Gaussian pulses below 10 ps with a beam quality parameter  $M^2 < 1.3$ . A third harmonic generation unit was employed for converting the central wavelength to 343 nm. A 103 mm  $f-\theta$  telecentric-lens was employed for beam focusing. The beam focus diameter was calculated to be 10  $\mu\text{m}$ . The resulting effective beam diameter and the sufficient depth of focus which the lens provides allow texturing surfaces with the desired feature sizes over large enough areas. Manipulation of the laser beam over the samples was performed by a two-mirror galvo scanner system with a positioning accuracy of 1  $\mu\text{m}$ .

This setup was employed for creating two different surface topographies, with different solid area ratios and increasing depths, in order to study geometrical effects on the LFP. One of the surface textures consisted of blind microholes ( $h$  in Table 1, see Figure 2), and the other one consisted of interconnected micropillars ( $p$  in Table 1, see Figure 2), both with different depths and heights, keeping the same spacing.

**Table 1. Geometric Dimensions and Processing Conditions of the Metallic Microstructures, Micropillars ( $p$ ), and Microholes ( $h$ ); Maximum Depth,  $\mu\text{m}$ ; Center to Center Spacing,  $\mu\text{m}$ ; Average Energy Per Pulse ( $E_p$ ),  $\mu\text{J}$ ; Scanning Speed, mm/s and Pulse to Pulse Laser Repetition Rate, kHz**

structure	depth ( $\mu\text{m}$ )	spacing ( $\mu\text{m}$ )	$E_p$ ( $\mu\text{J}$ )	speed (mm/s)	rep rate (kHz)
h1	3	17	0.35	1150	50
h2	6	17	0.35	1150	50
h3	9	17	0.35	1150	50
p1	10	17	0.35	400	400
p2	18	17	0.35	400	400
p3	26	17	0.35	400	400

The laser beam was focused on the surface and scanned over different areas following the desired paths. The employed average energy per pulse was adjusted to provide a fast laser ablation rate, while avoiding thermal damage to the sample. A regular orthogonal hatched pattern was used for creating the pillar-like structure, which arises from the material removal process. The beam speed and the laser repetition rate were set to provide a high pulse overlap during the material removal process.

The blind hole array was created by increasing the scanning speed while decreasing the laser repetition rate. This allows the spatial separation of the laser pulses. The separation between the scanned lines was selected to match the distance between the laser pulses along a track, limiting the interconnection between the resulting blind holes. A unidirectional hatched pattern was employed in this case. Both processes were repeated a number of times, to increase the depth of the resulting structures. In all experiments, the angle of incidence of

laser radiation was perpendicular to the specimen surface. The laser polarization was linear. The samples were irradiated in air, at room temperature. Processing conditions are summarized in Table 1. As can be observed in Figure 2, the shape of the microstructures is not rectangular with straight edges, which one can obtain with photolithographic techniques.

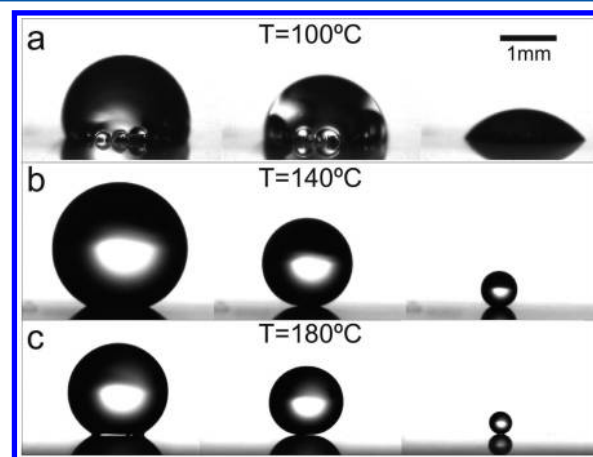


**Figure 1.** Snapshots of different stages of evaporating water droplets in heated micropillared structures: (a) Substrate at 100 °C, the droplet boils in 3 s. (b) Substrate at 140 °C, the droplet does not boil and survives for 40 s. (c) Substrate at 180 °C, the droplet survives for 120 s and the contact with the solid is at a minimum, which can be observed by the high contact angle, as well as by the light passing beneath the droplet.

## RESULTS AND DISCUSSION

The phenomenon reported in this paper was found when a micropillared surface was heated over the water-boiling temperature. At a typical temperature of 160 °C, a drop on a nonmachined flat area boils quickly, but when gently deposited on the heated micromachined area, the drop remains stable, steady, and almost spherical. A typical drop volume of 5  $\mu\text{L}$  will then take about 60 s to evaporate, while the same droplet will boil in a few seconds when deposited on the unmachined flat area. The temperature dependence can be observed in Figure 1. At room temperature, the contact angle with the solid is around 115°, and the droplet slowly evaporates. At boiling temperatures (typically 100 °C), the droplet boils within seconds. However, while increasing the temperature up to 140 °C, a critical change is observed. The droplet does not boil, its contact angle has increased (see Figure 4), and its evaporation time is 10 times longer than at boiling temperature. With increasing temperature, the contact angle keeps increasing (Figure 1 and Figure 4) approaching values close to 180°.

It is interesting to note that, when the critical temperature is reached, the drops stay steady in the same place where they have been deposited, up to the moment they are fully evaporated (see Figure 1). This behavior strongly contrasts with the classical Leidenfrost droplet, which normally drifts freely along the surface due to the lack of contact and friction. It is clear that there is some partial contact with the solid, which pins the drop and prevents it from drifting. When the surface was heated further to much higher temperatures, a classical Leidenfrost state was reached and the droplet moved freely over the surface.

Interestingly enough, Liu et al.<sup>13</sup> showed a similar effect in a very different type of microstructured surface. This demon-

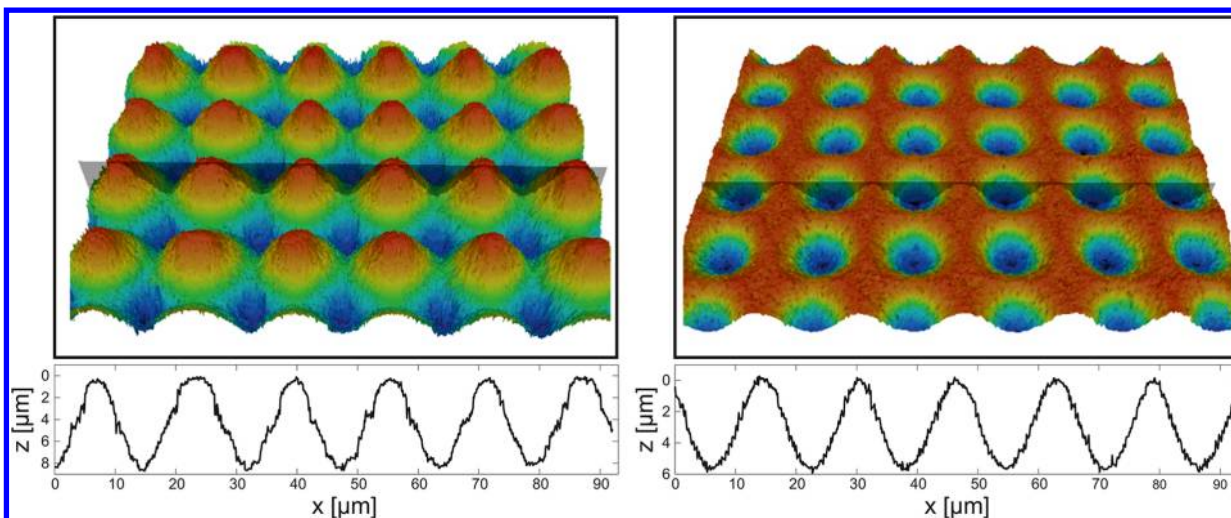


**Figure 2.** Confocal laser scanning microscope images of a pillar-like structure (left top) and a hole array structure (right top) with their respective cross section profiles, corresponding to samples *p2* and *h2* in Table 1.

states that the effect is more general and does not seem to depend on the particular geometry but mainly on the length scale of the pattern. In their work, they differentiated between a pinned Leidenfrost state and a pure unpinned one. In our case, the boundary between both states is too diffuse, and we will discuss this later.

Regarding the spurious contact with the structure, Kim et al.<sup>10</sup> reported intermittent contact with micro-obstacles in their experiments, as in the present case. The droplets were not completely steady but suffered some mild shivering. The film boiling regime was greatly disturbed, and the drops quickly vaporized when the intermittent contact was present. In spite of the partial contact with the solid observed in this work, no localized boiling has been observed in the droplet. In addition, the evaporating drops were fixed at distances well below one diameter with respect to its starting position.

A technique commonly used to accurately determine the LFP consists of measuring the evaporation time of droplets of the same volume at different temperatures. When the surface reaches the critical temperature, the evaporation time increases substantially, so the temperature at which the maximum evaporation time is found is considered to be the LFP.<sup>6</sup> However, in this study a more accurate method was employed to determine the LFP: by measuring the contact angle of the droplet with the surface at increasing temperatures.

As can be seen in Figure 4, a typical drop has an equilibrium contact angle of  $\sim 115^\circ$  at room temperature, when brought into contact with the surface. When the surface is heated, the contact angle does not change until the boiling regime is reached, around  $100^\circ\text{C}$ . Then, a contact angle cannot be properly defined, due to the appearance of bubbles inside the drop. When a critical temperature is reached, the droplet does not boil and its contact angle has sharply increased above  $115^\circ$  (see Figure 4, left). Depending on the surface structure, the temperature at this point was measured to be about  $140$  and  $160^\circ\text{C}$  (see Figure 3). With different pillar and blind hole structures, the determined critical temperature was quite reproducible with an accuracy of about 4%. Contact angles near  $180^\circ$  are achieved at sufficiently high temperatures (Figure 4). Due to the lack of contact, the drops start then drifting away from the machined areas.

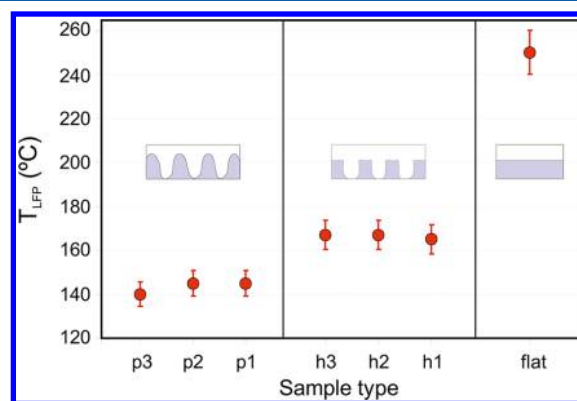


**Figure 3.** Leidenfrost points for the different surfaces tested: *p* stands for pillars, *h* for holes. The geometric characteristics of the surface features are summarized in Table 1.

We define then a pseudo-LFP as the temperature at which the droplet does not experience a sudden boiling, and a sharp increase in contact angle is observed (see Figures 1b and 4). The increase in contact angle with the temperature in the Leidenfrost regime is a manifestation of the partial contact with the solid, which is being gradually reduced as the temperature is further increased. The results of the measurements performed to determine the LFP on the different structures are summarized in Figure 3.

Due to such partial contact with the solid, the heat flux is still not at its minimum after the observed transition, and consequently, the evaporation time does not increase as much as in a classical Leidenfrost transition, where the droplet literally levitates and the heat flux reaches a minimum. For this reason, measuring evaporation times does not yield as accurate information on the transition as the contact angle does (see Figure 4).

The contact surface structures do not show profiles as sharp as those made with lithography, but rather smooth shapes with rounded edges. The main difference between *pillars* and *holes* is basically on the interconnection of the cavities; those in the pillared structure are interconnected, while those in the microholes are almost separated microcavities (Figure 2).



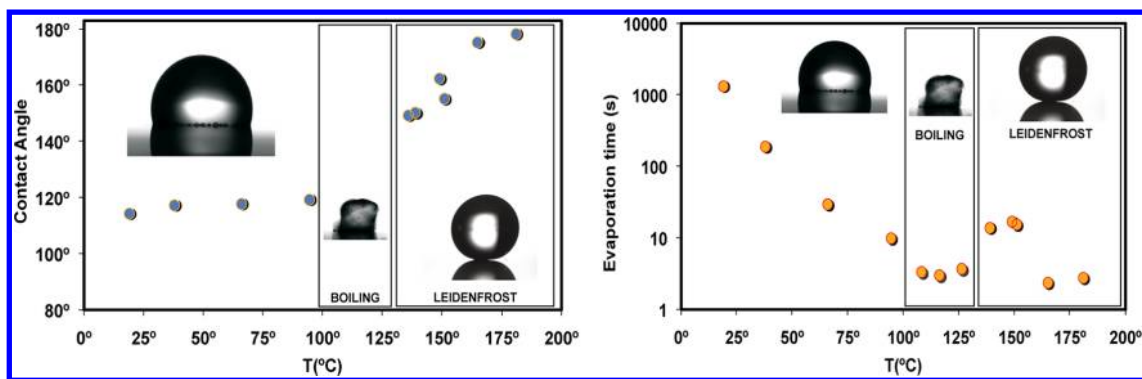


**Figure 4.** Contact angle and evaporation time of 3  $\mu\text{L}$  drops for different temperatures in different regimes for a pillar-like structure,  $p2$  in Table 1. The fact that the contact angle is below  $180^\circ$  and that the droplet is steady reveals a partial contact between the droplet and the structure at the Leidenfrost regime.

Bernardin and Mudawar<sup>19</sup> proposed a cavity activation model in which they used classical boiling theories to explain the formation and stability of the vapor film through the activation and growth of bubbles in the microscopic cavities of a surface. Applying the same model, we found that the cavities (with sizes between 5 and 10  $\mu\text{m}$ ) present in our sample surfaces are activated at temperatures as low as  $140^\circ\text{C}$ . However, this argument does not ensure the stability of the vapor film itself. Once the cavities are activated and the vapor bubbles are nucleated, they will grow and merge until a film is formed. If the vapor generation is fast enough, this will stabilize the film.

At this point, we can only give a qualitative argument for our results, but certainly more experiments and a theoretical explanation would be needed to support it. Focusing first on the pillared structure, it can be seen from Figure 2 that it basically consists of a network of interconnected micrometric cavities.

When water is in contact with such a structure at temperatures high enough for activation, bubbles will be generated in the cavities. If the formation is fast enough (i.e., if the temperature is high enough), a vapor bubble will quickly merge with its neighbors in a relatively organized way due to the structure and form a network of large bubbles. This may not form a homogeneous vapor film, but would be sufficient to overcome the pressure from the droplet (either capillary pressure or its weight, depending on the droplet size) and elevate it slightly over the surface minimizing the contact, which although reduced, it is still present. This might be the reason for the sudden increase in contact angle (Figure 4), which also implies that some contact is still present with the surface. Only when the temperature is high enough, is a complete and stable vapor film formed and the droplet literally floats over the surface, giving rise to contact angles of nearly  $180^\circ$ . In accordance with this qualitative analysis, it seems that the lack of sharpness in surface microstructures might be an advantage to stabilize the bubbles.

In the case of surface structures with microholes, due to the reduced connectivity, the temperature may have to be increased further to reach a similar state. In contrast to our results, in some studies<sup>3,5</sup> it has been demonstrated that rough surfaces present higher LFP. Those rough surfaces were produced by polishing the surface with abrasive particles of different sizes, which gives a highly random structure, with some preferred orientation. It seems that the bubble merging in surfaces showing sharp profiles is not so efficient as it is with an ordered and interconnected microstructure as presented here.

There are, however, quite unknown points that would require extended work and perhaps more sophisticated techniques. According to our calculations, the typical size of our structures might promote the formation of vapor bubbles, but we are not sure about the mechanism that helps to stabilize the partial vapor film for the different microstructures. In addition, it is not clear how the heat flux is altered by the presence of the microstructure, which might play a key role in the whole process.

## CONCLUSION

Micropatterned structures seem to be an excellent platform for stabilizing and merging vapor bubbles. A hybrid hydrophobic state has been identified, at much lower temperatures than the classical Leidenfrost temperature, in which the contact with the solid is substantially reduced, resulting in higher contact angles and longer droplet lifetimes. In such a state, liquid drops vaporize at the desired location, without drifting along the surface in frictionless motion. This is highly desirable for controlled evaporation processes in which the location of the deposits left by the droplet must be precisely controlled. Further research on structured surfaces can also be of interest for enhancing recently proposed drag reduction mechanisms,<sup>20</sup> by taking advantage of this pseudo-Leidenfrost state found at lower temperatures.

## AUTHOR INFORMATION

### Corresponding Author

\*E-mail: d.arnaldodelcerro@utwente.nl

### Notes

The authors declare no competing financial interest.

## REFERENCES

- (1) Leidenfrost, J. On the fixation of water in diverse fire (Duisburg, 1756). *Int. J. Heat Mass Transfer* **1966**, *9*, 1153–1166 reprint.
- (2) Gottfried, B.; Bell, K. Film Boiling of Spheroidal Droplets. Leidenfrost Phenomenon. *Ind. Eng. Chem. Fundam.* **1966**, *5*, 561–568.
- (3) Bernardin, J.; Mudawar, I. The Leidenfrost point: experimental study and assessment of existing models. *J. Heat Transfer* **1999**, *121*, 894–903.
- (4) Baumeister, K.; Simon, F. Leidenfrost temperature - Its correlation for liquid metals, cryogenics, hydrocarbons, and water. *J. Heat Transfer* **1973**, *95* (Ser C), 166–173.
- (5) Bernardin, J.; Stebbins, C.; Mudawar, I. Effects of surface roughness on water droplet impact history and heat transfer regimes. *Int. J. Heat Mass Transfer* **1996**, *40*, 73–88.

- (6) Biance, A.; Clanet, C.; Quéré, D. Leidenfrost drops. *Phys. Fluids* **2003**, *15*, 1632.
- (7) Tran, T.; Staat, H. J. J.; Prosperetti, A.; Sun, C.; Lohse, D. Drop impact on superheated surfaces. *Phys. Rev. Lett.* **2012**, *108*.
- (8) Bradfield, W. Liquid-solid contact in stable film boiling. *Ind. Eng. Chem. Fundam.* **1966**, *5*, 200–204.
- (9) Avedisian, C.; Koplík, J. Leidenfrost boiling of methanol droplets on hot porous/ceramic surfaces. *Int. J. Heat Mass Transfer* **1987**, *30*, 379–393.
- (10) Kim, H.; Truong, B.; Buongiorno, J.; Hu, L. On the effect of surface roughness height, wettability, and nanoporosity on Leidenfrost phenomena. *Appl. Phys. Lett.* **2011**, *98*, 083121.
- (11) Linke, H.; Alemán, B.; Melling, L.; Taormina, M.; Francis, M.; Dow-Hygelund, C.; Narayanan, V.; Taylor, R.; Stout, A. Self-propelled Leidenfrost droplets. *Phys. Rev. Lett.* **2006**, *96*, 154502.
- (12) Dupeux, G.; Clanet, C.; Hardt, S.; Quere, D. Viscous mechanism for Leidenfrost propulsion on a ratchet. *Bull. Am. Phys. Soc.* **2011**, *56*.
- (13) Liu, G.; Fu, L.; Rode, A.; Craig, V. Water droplet motion control on superhydrophobic surfaces: Exploiting the Wenzel-to-Cassie transition. *Langmuir* **2011**, *27*, 2595–2600.
- (14) Lagubeau, G.; Le Merrer, M.; Clanet, C.; Quéré, D. Leidenfrost on a ratchet. *Nat. Phys.* **2011**, *7*, 395–398.
- (15) Vakarelski, I.; Marston, J.; Chan, D.; Thoroddsen, S. Drag Reduction by Leidenfrost Vapor Layers. *Phys. Rev. Lett.* **2011**, *106*, 214501.
- (16) Sugiyama, Y.; Larsen, R.; Kim, J.; Weitz, D. Buckling and crumpling of drying droplets of colloid-polymer suspensions. *Langmuir* **2006**, *22*, 6024–6030.
- (17) Arnaldo del Cerro, D.; Römer, G.; Huis In't Veld, A. J. Erosion resistant anti-ice surfaces generated by ultra short laser pulses. *Physics Procedia* **2010**, *5*, 231–235.
- (18) Meijer, J.; Du, K.; Gillner, A.; Hoffmann, D.; Kovalenko, V. S.; Masuzawa, T.; Ostendorf, A.; Poprawe, R.; Schulz, W. Laser Machining by short and ultrashort pulses, state of the art and new opportunities in the age of the photons. *CIRP Annals - Manufacturing Technology* **2002**, *51*, 531–550.
- (19) Bernardin, J.; Mudawar, I. A cavity activation and bubble growth model of the Leidenfrost point. *J. Heat Transfer* **2002**, *124*, 864–874.
- (20) Tsai, P.; Peters, A. M.; Pirat, C.; Wessling, M.; Lammertink, R. G. H.; Lohse, D. Quantifying effective slip length over micropatterned hydrophobic surfaces. *Phys. Fluids* **2009**, *21*, 1–8.